Special Publication ARAED-SP-92002

THERMAL DECOMPOSITION OF ENERGETIC MATERIALS. 2. DEUTERIUM ISOTOPE EFFECTS AND ISOTOPIC SCRAMBLING IN CONDENSED-PHASE DECOMPOSITION OF OCTAHYDRO-1,3,5,7-TETRANITRO-1,3,5,7-TETRAZOCINE

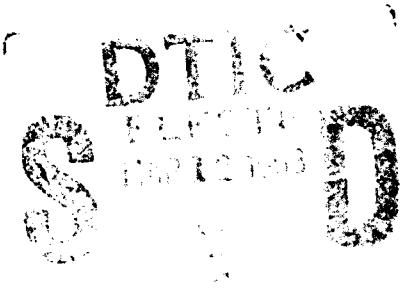

Richard Behrens, Jr.
Combustion Research Facility
Sandia National Laboratories
Livermore, CA 94551

Suryanarayana Bulusu
ARDEC

February 1993

U.S. ARMY ARMAMENT RESEARCH, DEVELOPMENT AND ENGINEERING CENTER

Armament Engineering Directorate

Picatinny Arsenal, New Jersey

The views, opinions, and/or findings contained in this report are those of the authors(s) and should not be construed as an official Department of the Army position, policy, or decision, unless so designated by other documentation.

The citation in this report of the names of commercial firms or commercially available products or services does not constitute official endorsement by or approval of the U.S. Government.

Destroy this report when no longer needed by any method that will prevent disclosure of its contents or reconstruction of the document. Do not return to the originator.

REPORT DOCUMENTATION PAGE

Form Approved OMB No. 0704-0188

1. AGENCY USE ONLY (Leave blank)	2. REPORT DATE	3. REPORT TYPE AND DATES COVERED
	February 1993	Technical

4. TITLE AND SUBTITLE

Thermal Decomposition of Energetic Materials. 2. Deuterium Isotope Effects and Isotope Scrambling in Condensed-Phase Decomposition of Octahydro-1,3,5,7-tetranitro-1,3,5,7-tetrazocine

5. FUNDING NUMBERS

6. AUTHOR(S)

Richard Behrens, Jr., Sandia National Laboratories
Suryanarayana Bulusu, ARDEC

7. PERFORMING ORGANIZATION NAME(S) AND ADDRESSES(S)

Combustion Research Facility
Sandia National Laboratories
Livermore, CA 94551

ARDEC, AED
Energetics & Warheads Div (SMCAR-AEE)
Picatinny Arsenal, NJ 07806-5000

8. PERFORMING ORGANIZATION REPORT NUMBER

Special Publication
ARAED-SP-92002

9.SPONSORING/MONITORING AGENCY NAME(S) AND ADDRESS(S)

ARDEC, IMD
STINFO Br (SMCAR-IMI-I)
Picatinny Arsenal, NJ 07806-5000

10. SPONSORING/MONITORING AGENCY REPORT NUMBER

11. SUPPLEMENTARY NOTES

12a. DISTRIBUTION/AVAILABILITY STATEMENT

Approved for public release; distribution is unlimited

12b. DISTRIBUTION CODE

13. ABSTRACT (Maximum 200 words)

The products formed in the thermal decomposition of octahydro-1,3,5,7-tetranitro-1,3,5,7-tetrazocine (HMX) have been traced to using mixtures of different isotopically labeled analogues of HMX. The isotopic analogues of HMX used in the experiments include ^{2}H, ^{13}C, $^{15}NO_2$, $^{15}N_{ring}$, and ^{18}O. The fraction of isotopic scrambling and the extent of the deuterium kinetic isotope effect (DKIE) are reported for the different thermal decomposition products. Isotopic scrambling is not observed for the N-N bond in N_2O and the C-H bonds in CH_2O. Only one of the C-N bonds in N-methylformamide (NMFA) undergoes isotopic scrambling. The lack of complete isotopic scrambling of the N-NO bond in 1-nitroso-3,5,7-trinitro-1,3,5,7-tetrazocine (ONTNTA) is shown to imply that some HMX decomposition occurs in the lattice. The behavior of the DKIE in different mixtures of isotopic analogues of HMX suggests that water probably acts as a catalyst in the decomposition. The results demonstrate that decomposition of HMX in the condensed phase has several reaction branches.

14. SUBJECT TERMS

DKIE, Isotope effect, Isotopic scrambling, HMX, NMFA, ONTNTA, Thermal decomposition

15. NUMBER OF PAGES
13

16. PRICE CODE

17. SECURITY CLASSIFICATION OF REPORT	18. SECURITY CLASSIFICATION OF THIS PAGE	19. SECURITY CLASSIFICATION OF ABSTRACT	20. LIMITATION OF ABSTRACT
UNCLASSIFIED	UNCLASSIFIED	UNCLASSIFIED	SAR

CONTENTS

Tables

Introduction

The cyclic nitramines octahydro-1,3,5,7-tetranitro-1,3,5,7-tetrazocine (HMX, I) and hexahydro-1,3,5-trinitro-*s*-triazine (RDX, II) are energetic ingredients that are used in various

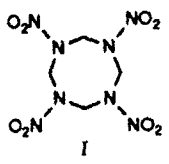

I

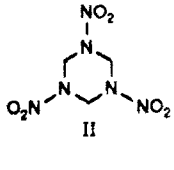

II

propellants and explosives. Understanding the complex physicochemical processes that underlie the combustion of these materials can lead to methods for modifying the propellant and explosive formulations in order to obtain better ignition, combustion, or sensitivity properties. Our work strives to provide a link between the physical properties and molecular structures of different nitramines and their combustive behavior. This requires the understanding of the reaction kinetics and transport processes in both the gas and condensed phases. The thrust of our work is to obtain a better understanding of physical processes and reaction mechanisms that occur in the condensed phase so that the identity and rate of release of the pyrolysis products from the condensed phase can be predicted, as a function of pressure and heating rate, based on the physical properties and molecular conformation of the material.

Reviews[1] of the literature on RDX and HMX have discussed the roles of unimolecular decomposition and autocatalysis on the thermal decomposition of these compounds. In addition, it has been shown that HMX decomposes in the condensed phase.[2-4] Recent simultaneous thermogravimetric modulated beam mass spectrometry (STMBMS) measurements[4] on the condensed-phase decomposition of HMX show that the identity and rates of release of the pyrolysis products are determined by complex physical processes coupled with several different chemical decomposition mechanisms. The physical processes include the formation and containment of the gaseous pyrolysis products in bubbles within the HMX particles and the subsequent release of the gases from within the bubbles as escape paths are formed within the HMX particles. The long containment time of initial decomposition products within the HMX particles allows secondary reactions within the gas bubbles. This sequence of physical processes and chemical reactions leads to the release of the following products during the decomposition of HMX: H_2O, HCN, CO, CH_2O, NO, N_2O, $(CH_3)_2NNO$, 1-nitroso-3,5,7-trinitro-1,3,5,7-tetrazocine (ONTNTA), amides (e.g., methylformamide), and a nonvolatile residue (NVR) that is a form of polyamide. The rates of release of the various pyrolysis products during these experiments are characteristic of solid-phase or autocatalytic reactions and show that the relative rates of formation vary during the course of the decomposition. These results along with deuterium kinetic isotope effect (DKIE) results[5,6] indicate that neither the least-energy pathway[7]

$$HMX \rightarrow NO_2 + H_2CN + 3H_2C{=}N{-}NO_2 \qquad (R1)$$

the concerted quadruple scission pathway

$$HMX \rightarrow 4H_2C{=}N{-}NO_2 \qquad (R2)$$

analogous to that found in IRMPD experiments with RDX,[8] nor the possible secondary reaction

$$H_2C{=}N{-}NO_2 \rightarrow CH_2O + N_2O \qquad (R3)$$

(1) For reviews see: (a) Boggs, T. L. The Thermal Decomposition Behavior of Cyclotrimethylene-trinitramine (RDX) and Cyclotetramethylene-tetranitramine (HMX). In *Fundamentals of Solid-Propellant Combustion*; Kuo, K. K., Summerfield, M., Eds.; Progress in Astronautics and Aeronautics, Vol. 90; AIAA Inc.: New York, 1984; p 121. (b) Fifer, R. A. Chemistry of Nitrate Ester and Nitramine Propellants. In *Fundamentals of Solid-Propellant Combustion*; Kuo, K. K., Summerfield, M., Eds.; Progress in Astronautics and Aeronautics, Vol. 90; AIAA Inc.: New York, 1984; p 177. (c) Schroeder, M. A. *Critical Analysis of Nitramine Decomposition Data: Product Distributions from HMX and RDX*; BRL-TR-2659; National Technical Information Service: Springfield, VA, 1985. (d) Schroeder, M. A. *Critical Analysis of Nitramine Decomposition Data: Activation Energies and Frequency Factors for HMX and RDX Decomposition*, BRL-TR-2673; National Technical Information Service: Springfield, VA, 1985.

(2) Bulusu, S.; Graybush, R. J. In *Proceedings of the 36th International Congress on Industrial Chemistry; Brussels, Belgium, 1967*; C. R. *Ind. Chim. Belge* **1967**, *32*, 647.

(3) Karpowicz, R. J.; Brill, T. B. *AIAA J.* **1982**, *20*, 1586.

(4) Behrens, Jr., R. *J. Phys. Chem.* **1990**, *94*, 6706 (part 1).

(5) Shackelford, S. A.; Coolidge, M. B.; Goshgarian, B. B.; Loving, B. A.; Rodgers, R. N.; Janney, J. L.; Ebinger, M. H. *J. Phys. Chem.* **1985**, *89*, 3118.

(6) Bulusu, S.; Weinstein, D. I.; Autera, J. R.; Velicky, R. W. *J. Phys. Chem.* **1986**, *90*, 4121.

(7) Melius, C. F. *J. Phys Colloq* **1987**, *48*, 341.

(8) Zhao, X.; Hintsa, E. J.; Lee, Y. T. *J. Chem. Phys.* **1988**, *88*, 801.

TABLE I: Experimental Parameters

compound	enrichment, %	experiment[a] 1	2	3	4	5	6	7
HMX-ul		8.60		4.20	4.06	4.40		
HMX-d_8	100		7.69	4.29	3.79			
HMX-^{13}C	47.6						3.27	3.23
HMX-$^{15}N_{ring}$	99							3.77
HMX-$^{15}N_8$	99					4.40		
HMX-^{18}O	4.94						2.89	
temp,[b] °C				234.7	234.7	237.1	233.5	232
ramp time,[c] s				2800	2800	3000	3000	2860
decomp time,[c] s		8000	13400	12800	10900	7200	8500	
mixing[d]				M	S	S	S	S

[a] The amount of each isotopomer used in each experiment is listed in milligrams. [b] Isothermal temperature of experiments. [c] Ramp time is the time from the start of the experiment to attainment of the isothermal temperature, and the decomposition time is the time from attainment of the isothermal temperature until the sample stops releasing gaseous products. [d] M = physically mixed sample; S = mixed in acetone solution.

can completely explain the condensed-phase decomposition of HMX.

In this study, we use mixtures of isotopically labeled compounds to track the breaking and formation of chemical bonds that lead to the generation of pyrolysis products from the thermal decomposition of HMX. We also use the DKIE to probe the role of hydrogen in the formation of the different decomposition products. We present results from STMBMS measurements with mixtures of unlabeled HMX and the following isotopically labeled analogues: HMX-d_8, HMX-^{13}C, HMX-$^{15}N_{ring}$, HMX-$^{15}N_8$, and HMX-^{18}O. The STMBMS measurements are used to determine the DKIE on the pyrolysis products during the course of the decomposition. They are also used to determine the amount of isotopic scrambling that occurs in forming the pyrolysis products from different isotopic mixtures of HMX. We report the fraction of isotopic scrambling for most of the products formed in experiments with mixtures of different combinations of the labeled HMX compounds.

Experimental Section

Instrument Description. The STMBMS apparatus and basic data analysis procedure have been described previously.[9,10] This instrument allows the concentration and rate of formation of each gas-phase species in a reaction cell to be measured as a function of time by correlating the ion signals at different m/z values measured with a mass spectrometer with the force measured by a microbalance at any instant. In the experimental procedure, a small sample (~10 mg) is placed in an alumina reaction cell that is then mounted on a thermocouple probe that is seated in a microbalance. The reaction cell is enclosed in a high-vacuum environment ($<10^{-6}$ Torr) and is radiatively heated by a bifilar-wound tungsten wire on an alumina tube. The molecules from the gaseous mixture in the reaction cell exit through a small-diameter (~0.01 cm in these experiments) orifice in the cap of the reaction cell and traverse two beam-defining orifices before entering the electron-bombardment ionizer of the mass spectrometer where the ions are created by collisions of 18-eV electrons with the different molecules in the gas flow. The background pressures in the vacuum chambers are sufficiently low to eliminate significant scattering between molecules from the reaction cell and background molecules in the vacuum chambers. The different m/z value ions are selected with a quadrupole mass filter and counted with an ion counter. The gas flow is modulated with a chopping wheel, and only the modulated ion signal is recorded. The containment time of gas in the reaction cell is a function of the orifice area, the free volume within the reaction cell, and the characteristics of the flow of gas through the orifice. For the reaction cell used in the experiments with HMX, the time constant for exhausting gas from the cell is small (~0.2 s) compared to the duration of the experiments (>~1000 s). Note that the containment time of gas within the reaction cell is short once the gas molecules are in the free volume of the cell, but it may be much longer if the gas is trapped in the condensed phase of the material within the cell. For studying reactions that occur within the condensed phase, the reaction cell allows the surface regression rate of the particles due to evaporation to be controlled by adjusting the area of the exhaust orifice. In this way a balance is achieved between the rate of product formation within the particles and the rate of release of gaseous products from the particles.

Sample Preparation. Samples of HMX with different isotopic labels were synthesized by the general method previously reported elsewhere.[11] To obtain a given isotopic analogue, starting materials with the appropriate isotopic enrichment were employed. Briefly, the synthesis involves treating hexamine in solution of acetic anhydride and glacial acetic acid maintained at 44 °C with a "nitrolysis" mixture consisting of ammonium nitrate and 98–100% nitric acid. This reaction yields a mixture of HMX and RDX, and the workup requires separation of the two products by extraction with ethylene dichloride in which RDX is much more soluble than HMX. Each product is then purified by multiple recrystallizations from aqueous acetone and characterized by melting points, ^1H NMR, and mass spectra.

The ^{15}N-labeling in the HMX ring is achieved by first synthesizing hexamine from $(CH_2O)_n$ and $^{15}NH_3$ (liberated from ammonium acetate and 30% aqueous KOH) and using $^{15}NH_4NO_3$ in the nitrolysis mixture. Nitro-^{15}N labeling requires the use of $NH_4{}^{15}NO_3$ and $H^{15}NO_3$, with the latter prepared by vacuum distillation at low temperature from $Na^{15}NO_3$ and cp H_2SO_4. ^{13}C-enrichment uses $(^{13}CH_2O)_n$ as starting material for hexamine while ^{18}O-labeling requires $NH_4N^{18}O_3$ and $HN^{18}O_3$ obtained as above. Deuterium labeling is achieved by starting from hexamine-d_{12} and employing CH_3COOD in the reaction.

The isotopic enrichment of each of the isotopomers used in the experiments is listed in Table I.

Experiments are conducted on samples prepared by mixing the ingredients both mechanically and in an acetone solution. The samples mixed in the acetone solution are prepared by dissolving approximately equal quantities of the two isotopomers in solution and then letting the solvent evaporate. The mechanically mixed samples were prepared by mixing equal amounts of the two isotopomers in the reaction cell. The median particle size of the HMX used in the experiments with mechanically mixed samples is 40 μm. The amounts of each ingredient used in each experiment are listed in Table I.

For each mixed-isotope experiment listed in Table I, experiments were run on each of the isotopic analogues separately. The results from these experiments are used to check for the presence of ion signals at m/z values that should originate only from the mixing of isotopes in the scrambling experiments. If there is a measurable

(9) (a) Behrens, Jr., R. *Rev. Sci. Instrum.* **1986**, *58*, 451. (b) Behrens, Jr., R. The Application of Simultaneous Thermogravimetric Modulated Beam Mass Spectrometry and Time-of-Flight Velocity Spectra Measurements to the Study of the Pyrolysis of Energetic Materials. In *Chemistry and Physics of Energetic Materials*; Bulusu, S. N., Ed.; Proceedings of the NATO Advanced Study Institute, Vol. 309; Kluwer Academic Publishers: Dordrecht, The Netherlands, 1990; p 327.

(10) Behrens, Jr., R. *Int. J. Chem. Kinet.* **1990**, *22*, 135.

(11) Bulusu, S.; Autera, J. R.; Axenrod, T. *J. Labelled Compd. Radiopharm.* **1980**, *17*, 707.

amount of ion signal present in the experiments with the separate isotopic analogues, then the results of the separate experiments are used to correct the data from the isotope scrambling experiments.

Analysis

The data analysis procedures used for identifying the pyrolysis products and determining their rates of formation have been described previously.[9,10,12] Since this paper examines the extent of isotopic scrambling and the DKIE on the relative rates of formation of the various products, it is sufficient to compare the ratios of the ion signals measured at different m/z values for the various products. The structures of the more complex decomposition products discussed in this paper are reasonably assumed structures based on the mass spectra of different isotopic analogues of HMX.[10] The assumed structures of two of the products, $(CH_3)_2NNO$ and $(CH_3)_2NCHO$, were shown to be formed during the decomposition of RDX in experiments using tandem mass spectrometry.[13]

The relative size of the ion signals at the different m/z values associated with an individual decomposition product is dependent on the amount of each isotopically labeled analogue used in the experiment, the fraction of each analogue that participates in forming isotopically scrambled products, the cracking factors in the ion fragmentation process, and the fraction of isotopic enrichment in each isotopically labeled analogue.

The amount of each product isotopomer formed from the decomposition of a mixture of r moles of isotopomer 1 and s moles of isotopomer 2 of HMX is given by

$$r\mathrm{HMX}_1 + s\mathrm{HMX}_2 \rightarrow x\kappa r(1-f)\mathrm{A}_{11} + \kappa s(1-f)\mathrm{A}_{22} + \kappa f(xr+s)\mathrm{A}_{12} \quad \text{(R4)}$$

where A represents the type of pyrolysis product, A_{11} and A_{22} are formed from HMX_1 and HMX_2, respectively, A_{12} represents the set of mixed isotope products, κ is the number of moles of product A formed per mole of HMX_2, x is the ratio of the number of moles of product A formed from HMX_1 to the number of moles of product A formed from HMX_2 (for deuterium-labeled HMX this corresponds to the DKIE factor), and f is the fraction of the product molecules produced from either HMX_1 or HMX_2 that participate in isotope scrambling. For experiments in which the isotopomers are not completely labeled, reaction R4 is modified to account for the fraction of enrichment of each of the isotopomers used in the scrambling experiment. The predicted combinations of the isotopes of the different elements in each of the mixed-product isotopomers are assumed to be random over the available molecular configurations.

After the expression for the amount of different product isotopomers is determined, it is combined with the following expression that accounts for the relative number of ions formed in the mass spectrometer at different m/z values from the product isotopomer

$$S_k^+ = \sum_{i=1}^{\text{no. of isotopomers}} F_{i,k}A_i^+ \qquad (1)$$

where S_k^+ is the ion signal at $m/z = k$, A_i^+ is the total number of ions formed from the isotopomer A_i with mass m_i, and $F_{i,k}$ is the fraction of the total number of ions formed from A_i that appear at $m/z = k$. The $F_{i,k}$ terms are assumed to be independent of the isotopic mass in the product molecules except for the case in which the ion fragmentation involves the scission of a bond with a hydrogen isotope. For the hydrogen bond breaking cases separate fragmentation terms $F_{i,k}$ are used for each product isotopomer.

Based on reaction R4, eq 1, and the isotopic enrichment fractions for the HMX analogues used in the experiments, expressions for the amount of ion signal at each different m/z value associated with a decomposition product are formulated. These expressions are then used to construct equations based on the ratios of the ion signals at different m/z values for a given product. These equations are then solved for the values of f and x.

Prior to using the data from the isotopic scrambling experiments to determine the values of f and x, the ion signals at m/z values in which isotopic scrambling is expected are corrected for ion signals that may be present from a source other than the product of interest. The correction is accomplished by determining the ratio of the unexpected signal at the desired m/z value to the signal from the HMX $m/z = 120$ fragment (or the corresponding isotopic analogue) from experiments with individual isotopic analogues and applying the correction factor to the results from the isotopic scrambling experiment.

TABLE II: H_2O Isotopic Scrambling Results

isotope	expt	m/z	rel intensities[a]	temporal correlation[b]
H/D	3	18	100	N
		19	144	N
		20	53	N
	4	18	100	N/Y
		19	126	N/Y
		20	46	N/Y

[a] The errors in these values are less than ±2%. [b] For the entries with N/Y the signals are not correlated in the induction stage but are correlated in the acceleratory and decay stages.

TABLE III: CH_2O Isotopic Scrambling Results

isotopes	expt	m/z	rel intensities[a]	temporal correlation
H/D	3	29	34.7	N
		31	10.7[b]	N
		32	100	N
	4	29	44.8	Y
		31	10.3[b]	Y
		32	100	Y
$^{13}C/^{18}O$	6	31	100	Y
		32	7.47 ± 0.45	Y
		33	1.66 ± 0.38[c]	Y

[a] The errors on all data without specific error values are ±2%. The relative intensities for ion signals lacking temporal correlation are given at the maximum value in the experiment. [b] Corrected for 31^+ contribution from pure HMX-ul. [c] Corrected for the 33^+ contribution observed in separate experiments with ^{13}C-labeled and ^{18}O-labeled HMX. The corrections are normalized by using the isotopic analogue of the nominal $m/z = 120$ peak observed in HMX-ul.

TABLE IV: N_2O Isotopic Scrambling Results

isotope	expt	m/z	rel intensities[a]	temporal correlation
$^{15}N_\beta/^{14}N_\beta$	5	44	100	Y
		45	9.7	Y
		46	94.3	Y

[a] The ion signal at each m/z value is corrected for contributions not arising from N_2O in the pure $^{15}N_\beta$ and $^{14}N_\beta$ HMX samples. The corrections are normalized for the mixed-isotope experiment using the isotopic analogue of the HMX $m/z = 120$ peak. The errors in these values are less than ±2%.

Results

The temporal behaviors of the ion signals at several m/z values from representative isotopic scrambling experiments are shown in Figures 1–4 for H_2O, CH_2O, N_2O, and ONTNTA, respectively. The time that the sample first attains its isothermal temperature is listed in Table I. There is a high degree of temporal correlation between the ion signals at different m/z values for H_2O, CH_2O, and N_2O and a lower degree of correlation between the ion signals at the m/z values for ONTNTA. The relative intensities of the ion signals at various m/z values associated with H_2O, CH_2O, N_2O, $(CH_3)NHCHO$, $(CH_3)_2NNO/(CH_3)_2NCHO$, and ONTNTA for the different isotopic scrambling experiments are listed in Tables II–VII, repectively. The results of the analysis

(12) Behrens, Jr., R. *Int. J. Chem. Kinet.* **1990**, *22*, 159.
(13) Snyder, A. P.; Kremer, J. H.; Liebman, S. A.; Schroeder, M. A.; Fifer, R. A. *Org. Mass Spectrom.* **1989**, *24*, 15.

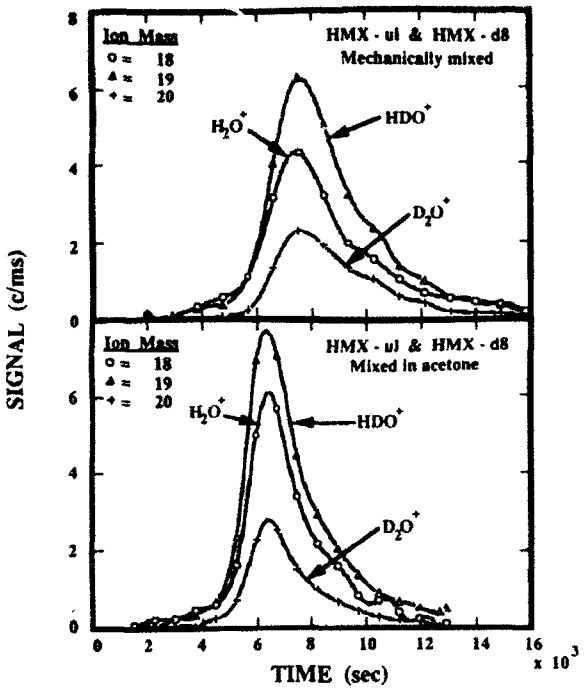

Figure 1. Ion signals from water products formed during the decomposition of unlabeled HMX and HMX-d_8 in isotopic scrambling experiments 3 (top) and 4 (bottom).

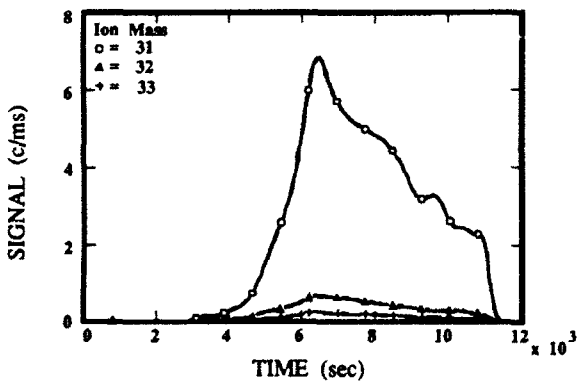

Figure 2. Ion signals from formaldehyde products formed during the decomposition of HMX-^{13}C and HMX-^{18}O in isotopic scrambling experiment 6.

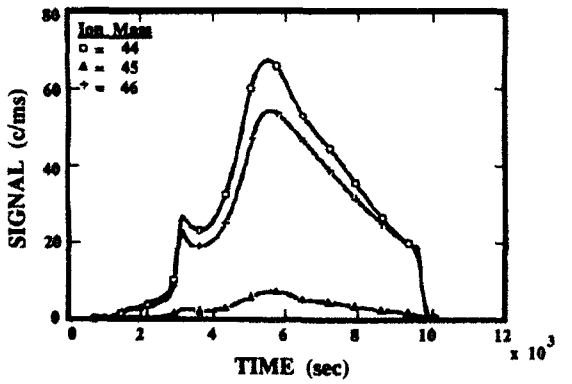

Figure 3. Ion signals from N_2O products formed during the decomposition of unlabeled HMX and HMX-$^{15}N_8$ in isotopic scrambling experiment 5.

to determine the fraction of the HMX isotopic analogues that participate in isotopic scrambling to produce mixed-isotope products and the extent of the DKIE for the different products are listed in Table VIII.

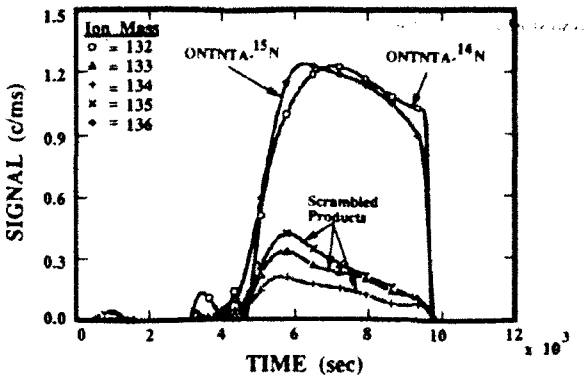

Figure 4. Ion signals from the ONTNTA products formed during the decomposition of unlabeled HMX and HMX-$^{15}N_8$ in isotopic scrambling experiment 5. The ion signals have been corrected for the contribution from HMX ion fragments but not ion signals that originate from decomposition of the nonvolatile residue.

TABLE V: CH_3NHCHO Isotopic Scrambling Results

isotope	expt	m/z	rel intensities[a]	temporal correlation
$^{13}C/^{15}N_{ring}$	7	58	56	Y
		59	100	Y
		60	56	Y
		61	16.3 ± 0.8[b]	Y
		62	0.3 ± 0.3[b]	Y

[a]The errors on all data without specific error values are ±2%. [b]The ion signal has been corrected for contributions not arising from CH_3-NHCHO.

TABLE VI: $(CH_3)_2NNO$ and $(CH_3)_2NCHO$ Isotopic Scrambling Results

isotopes	expt	m/z	rel intensities[a]	temporal correlation[b]
H/D	3	73	17	G1
		74	41	N
		75	100	G1
		76	72	G2
		77	89	G2
		78	82	N
		79	33	G2
		80	29	N
H/D	4	73	31	Y
		74	63	Y
		75	78	Y
		76	88	Y
		77	100	Y
		78	95	N
		79	36	Y
		80	18	N
$^{13}C/^{15}N_{ring}$	7	73	21	
		74	97	
		75	100	
		76	45	
		77	5	

[a]The errors on all data without specific error values are ±2%. [b]Y indicates that the m/z values are correlated with all the other m/z values that are listed for an experiment. G1 and G2 are groups of correlated masses within one experiment.

H_2O. Scrambling of the hydrogen isotopes *is observed* in the formation of water from experiments in which the HMX-unlabeled (ul) and HMX-d_8 were mixed both mechanically and in solution. The data from both experiments are shown in Figure 1. Values of f of 0.99 for water formed from the mechanically mixed powders and 0.93 for water formed from samples mixed in solution (see Table VIII) indicate that the hydrogen and deuterium are completely and randomly exchanged prior to release from the reaction cell. The result from the mechanically mixed sample indicates that the exchange takes place after the water leaves the HMX particles. Since a low electron energy of 18 eV is used in the mass

TABLE VII: ONTNTA Isotopic Scrambling Results

isotopes	expt	m/z[a]	rel intensities[b]	temporal correlation[c]
H/D	3	132	64 ± 14	Y
		133	10 ± 1	Y
		134	0	Y
		135	9 ± 1	
		136	100 ± 3	
	4	132	71 ± 14	Y
		133	5 ± 1	Y
		134	0	Y
		135	7 ± 1	
		136	100 ± 3	
$^{15}N_8$/ul	5[d]	132	100	G1
		133	14	G2
		134	0	G2
		135	20	G2
		136	85	G1
	5[e]	132	100	G1
		133	13	G2
		134	0	G2
		135	14	G2
		136	99	G1

[a] The m/z values are for an ion formula of $C_2H_4N_2(NO)(NO_2)$. [b] The relative intensities for each ion have been corrected for the HMX contribution to the m/z value and also any contribution at the scrambled m/z values that originate from only the pure isotopic analogue. The errors on all data without specific error values are ±2%. The larger errors for m/z = 132 in the H/D experiments are due to the large correction for the $C_3D_4N_3(NO_2)$ ion fragment from HMX-d_8. [c] Y indicates that the m/z values are correlated with all the other m/z values that are listed for an experiment. G1 and G2 are groups of correlated masses within one experiment. [d] Data at 6000 s. [e] Data at 8000 s.

TABLE VIII: Mixing Fractions and DKIE Results from Isotopic Scrambling Experiments

decomposition product	scrambling isotopes	mixing[a]	mixing fraction f	DKIE x[b]
H_2O	H/D	M	0.99 ± 0.04	2.24 to 1.0[c]
	H/D	S	0.93 ± 0.04	1.36 ± 0.02
CH_2O	H/D	M	0.06 ± 0.01 to 0.07 ± 0.01	0.88 ± 0.01 to 1.49 ± 0.01
	H/D	S	0.06 ± 0.01	1.03 ± 0.01 to 1.07 ± 0.01
	$^{13}C/^{18}O$	S	0.80 ± 0.20	
N_2O	$^{15}N_8/^{14}N_8$	S	0.049 ± 0.005	
CH_3NHCHO	$^{13}C/^{15}N_{ring}$	S	0.85 ± 0.15/ 0.04 ± 0.06[c]	
ONTNTA	H/D	M	0.44 ± 0.10	0.61 ± 0.10
	H/D	S	0.26 ± 0.08	0.90 ± 0.18
	$^{15}N_8/^{14}N_8$	S	0.25 ± 0.01/ 0.37 ± 0.01[d]	
	$^{15}N_8/^{14}N_8$	S	0.24 ± 0.01/ 0.24 ± 0.01[d]	

[a] M = mechanical mixing; S = mixed in acetone solution. [b] The values of x are calculated only for the H/D-exchange experiments. [c] The 0.85 value is based on the ion signal ratio of the $61^+/60^+$ m/z values, and the 0.05 value is based onthe ion signal ratio of the $62^+/61^+$ m/z values. This difference is indicative of only one of the C–N bonds breaking during the formation of CH_3NHCHO. [d] The first value listed is based on the ion signal ratio of the $133^+/132^+$ m/z values, and the second value listed is based on the ion signal ratio of the $135^+/136^+$ m/z values. The 0.25/0.37 and 0.24/0.24 values are based on the data shown in Table VII taken at 6000 and 8000 s, respectively. [e] The ratio of the H_2O to D_2O produced during this experiment varies from 2.24 at the start of the acceleratory stage down to 1.0 near the end of the decay stage.

spectrometer, contribution from OD^+ is ignored. The results are calculated assuming that only the molecular ions H_2O^+, HDO^+, and D_2O^+ contribute to the measured signals.

The temporal behaviors of the water signals show several interesting features. In the results shown in Figure 1, both experiments were conducted at the same isothermal temperature and both attained the isothermal temperature at the same time from the start of the experiment. The experiment with the mechanically mixed HMX-ul and HMX-d_8 *does not exhibit temporal correlation* between the H_2O^+, HDO^+, and D_2O^+ signals throughout the decomposition. The H_2O^+ and HDO^+ signals are higher with respect to the D_2O^+ during the induction and acceleratory stages of the reaction than during the decay stage. The DKIE value for x varies from 2.24 at the start of the acceleratory stage, to 1.37 at the peak, and down to 1.0 near the end of the decay stage. In contrast, the experiment with the HMX-ul and HMX-d_8 mixed in solution *exhibits a high degree of temporal correlation* between the H_2O^+, HDO^+, and D_2O^+ signals through the acceleratory and decay stages but lacks temporal correlation in the induction stage. The DKIE value for x throughout the correlated region is 1.37. Furthermore, a comparison between the water signals from the samples mixed in solution and those mixed mechanically shows that the water generated from the sample mixed in solution evolves sooner and more rapidly after attaining the isothermal temperature than the water generated from the sample mixed mechanically. In addition, the decomposition times listed in Table I show that the unlabeled HMX decomposes in a shorter time than the deuterium-labeled HMX and that the experiments with mixture of HMX-ul and HMX-d_8 have decomposition times between those for the pure HMX-ul and HMX-d_8. Furthermore, the results in Table I show that the HMX-ul and HMX-d_8 mixed in solution decomposes in a shorter time than the HMX-ul and the HMX-d_8 that is mechanically mixed.

CH_2O. As indicated in Table VIII, the fraction of HMX that forms formaldehyde with hydrogen and deuterium exchange is about 6% for the experiments in which the samples are mixed either mechanically or in solution. Experiment 3 with HMX-ul/HMX-d_8 mixed mechanically lacks temporal correlation (see Table III) between the ion signals from the different isotopic analogues of formaldehyde. The DKIE for experiment 3 ranges from 1.49 at the start of the decomposition down to 0.88 near the end of the decomposition. In contrast, experiment 4 with the HMX-ul/HMX-d_8 mixed in solution exhibits both a high degree of temporal correlation between the ion signals from the isotopic analogues of formaldehyde and a DKIE for formaldehyde that ranges between 1.03 and 1.07 during the entire experiment. The ion signals used in the analysis are for m/z values of CH_2O^+, CHO^+, and their isotopic analogues. Measured ion fragmentation factors for CH_2O and CD_2O were used to calculate the ratio of CHO^+/CH_2O^+ and CDO^+/CD_2O^+ formed in the ionization process.

Experiment 6 with a mixture of HMX-^{13}C and HMX-^{18}O shows that 80% of the formaldehyde formed is from mixing between the two differently labeled HMX analogues. The higher error in this mixing fraction result is due to the lower amounts of isotopic enrichment in the starting HMX materials. The ion signals of $^{13}CH_2O$ (31), $CH_2{}^{18}O$ (32), and $^{13}CH_2{}^{18}O$ (33) were used to calculate the value for f.

N_2O. Experiment 5 (Table IV) with a mixture of HMX-ul and HMX-$^{15}N_8$ shows that only 5% of the N_2O is formed from mixing between the two differently labeled HMX analogues. The ion signals of $^{14}N_2O^+$, $^{14}N^{15}NO^+$, and $^{15}N_2O^+$ are used to calculate the mixing fraction.

CH_3NHCHO. Experiment 7 with a mixture of HMX-^{13}C and HMX-$^{15}N_{ring}$ shows that one of the C–N bonds in the *N*-methylformamide (NMFA) molecule participates in mixing between the two isotopic HMX analogues 85 ± 15% of the time, whereas both C–N bonds participate in the mixing only 5 ± 6% of the time. These results are based on the ion signals at m/z values of 60, 61, and 62. These three m/z values have contributions from the isotopic analogues of the CH_3NHCHO^+ and CH_3NCHO^+ ions formed from *N*-methylformamide. Using the ratio of the ion signals at m/z values of 62 and 61 allows the relative amount of $^{13}CH_3{}^{15}NH^{13}CHO$ formed to be calculated. This species can be formed during the experiment only by having both C–N bonds participate in the reaction. The results show that this occurs only 5 ± 6% of the time. On the other hand, using the ratio of the ion signals at m/z values of 61 and 60 allows the formation of either the $^{13}CH_3{}^{15}NHCHO$ or $CH_3{}^{15}NH^{13}CHO$ products to be investigated. These two products involve the participation of only one of the C–N bonds in the reaction. The

results show that 85 ± 15% of the NMFA is formed from reactions between the two different isotopic analogues that *involve scrambling* of only *one* C–N bond. However, the results cannot distinguish between the two possible isotopic conformations. In addition, the high degree of temporal correlation between the ion signals at the different NMFA m/z values indicates that decomposition reactions involving the C–N bonds are not changing during the course of the decomposition.

Experiments 3 and 4 with mixtures of HMX-ul and HMX-d_8 show that there is exchange of hydrogen and deuterium during the formation of NMFA. However, since the nonvolatile residue that is formed during the decomposition slowly decomposes along with the remaining HMX, there are small ion signals at many different m/z values that are due to the decomposition of the NVR. The region of m/z values between 52 and 58 contains small signals that are 10–20% of the size of the NMFA signals. Consequently, since the stoichiometry of these ions is not known, it is not possible to correct for their contributions to the ion signals in the m/z region of 58–64 that may arise from their deuterium analogues. Therefore, it is not possible to determine the mixing fraction and the DKIE values for CH_3NHCHO from the results.

$(CH_3)_2NNO$ and $(CH_3)_2NCHO$. The results from experiments 3 and 4 with mixtures of HMX-ul and HMX-d_8 and from experiment 7 with HMX-^{13}C and HMX-$^{15}N_{ring}$ are listed in Table VI. The presence of ion signals at the m/z values between the m/z values for $(CH_3)_2NNO$ and $(CH_3)_2NCHO$ from pure unlabeled HMX (73, 74) and the pure deuterium-labeled HMX (80) clearly shows that the hydrogen isotopes scramble during the formation of $(CH_3)_2NNO$ and $(CH_3)_2NCHO$. The presence of a small ion signal at $m/z = 77$ in experiment 7 indicates that at least one of the products is formed with complete rearrangement of all the C–N bonds. Since ion signals occur at the same m/z values for both of the decomposition products, the fraction of each product that arises from mixing of the isotopic analogues cannot be extracted from the data.

ONTNTA. The results from experiments 3 and 4 with mixtures of HMX-ul and HMX-d_8 and from experiment 5 with HMX-ul and HMX-$^{15}N_8$ are listed in Table VII. The results for the *mechanically mixed sample* in the experiment with hydrogen isotopes show that 44 ± 10% of the ONTNTA comes from reactions *between* the HMX molecules and the remainder originates from *individual* HMX molecules. The mechanically mixed sample also exhibits an inverse DKIE with $x = 0.61 \pm 0.10$. The results from the experiment with the sample mixed in solution show that 26 ± 8% of the ONTNTA comes from reactions *between* the HMX molecules and the remainder is from individual molecules. The sample mixed in solution has a value of x of 0.9 ± 0.18. The high error on this result precludes an estimate of the DKIE for this experiment. The fact that there is not significant signal at $m/z = 134$ (indicating the presence of two hydrogen and two deuterium atoms on the ONTNTA ion fragment) shows that only one of the hydrogen atoms on the HMX participates in the reaction that forms ONTNTA.

The ion signals at m/z values from 132 to 136, measured in the experiment with HMX-ul and HMX-$^{15}N_8$ and corrected for any HMX ion fragmentation contribution, are shown in Figure 4. The relative intensities of the ion signals at the m/z values of 132–136, after being corrected for ion signals originating from products associated with the NVR, are listed in Table VII. As can be seen from Figure 4, the ion signals are not all temporally correlated. Therefore, the fraction of ONTNTA formed from mixed isotopes is calculated at two different times during the decomposition. At 6000 s two different values for the fraction of mixing were obtained. The values for the fraction of mixing are 0.25 using the ratio of ion signals at m/z values of 133 and 132 and 0.37 using the ratio of ion signals at m/z values of 135 and 136. At 8000 s the value for the fraction of mixing is 0.24 using the ion signal ratios at m/z values of 133/132 or 135/136.

Discussion

The results from our isotopic scrambling and DKIE studies provide insight into the reaction paths and rate-controlling steps for the decomposition of HMX. They also illustrate the limitations of using isotopically labeled analogues to determine the reaction pathways. Products that show little or no isotopic scrambling provide more definitive information than products that undergo significant isotopic scrambling. For example, if the product contains a mixture of isotopes, then the scrambling may have occurred either during the initial formation of the product or after it was formed but prior to detection. Thus, scrambling of the isotopes in a given product after its initial formation limits the amount of mechanistic information obtained in the experiment.

In our experiments, only a small amount of isotopic scrambling (<6%) is observed for the hydrogen atoms in formaldehyde, the nitrogen atoms in N_2O, and one of the C–N bonds in NMFA. All of the other products undergo various amounts of isotopic scrambling.

There is little isotopic scrambling in the N_2O product formed from HMX-ul and HMX-$^{15}N_8$. This is consistent with previous work[14] on the decomposition of mixtures of HMX-ul and HMX-$^{15}NO_2$ that also found no isotopic scrambling in the N_2O product. However, if the N_2O is formed from a HMX-ul/HMX-$^{15}NO_2$ mixture by rupture of the N–N bond and the subsequent reaction of the NO_2 with a product formed from the ring nitrogen, then no scrambling of the nitrogen in N_2O will be observed even though the N–N bond ruptured. On the other hand, if the N–N bond breaks in the experiments with HMX-ul and HMX-$^{15}N_8$, then the N_2O product must contain mixed isotopes. Thus, the results with HMX-ul/HMX-$^{15}N_8$ show more conclusively that the N_2O formed in the decomposition originates directly from the HMX molecule without N–N bond breaking.

The lack of isotopic scrambling in the formation of N_2O suggests that HMX may decompose by formation of a four-membered-ring transition state leading to the formation of N_2O and CH_2O. However, previous quantitative results[4] on the rates of formation of products from the decomposition of HMX, under conditions similar to those in the experiments presented here, show that only 3 mol of N_2O is formed per mole of HMX. Thus, one N–N bond in HMX may break and lead to the formation of nitrogen-containing products other than N_2O. Both the lack of isotopic scrambling and the quantitative results for N_2O support the mechanism of reactions R1 and R3 in which the N–N bond breaks forming NO_2 and the HMX ring unravels forming the H_2CN radical and three molecules of both N_2O and CH_2O, possibly through decomposition of three methylenenitramine precursors. Thus, the lack of isotopic scrambling in the N_2O product is consistent with a decomposition mechanism other than oxygen atom transfer through a four-membered-ring transition state. If HMX does decompose to N_2O and formaldehyde through the methylenenitramine intermediate, then the product distribution is different from that measured for methylenenitramine decomposition in molecular beam infrared multiphoton dissociation (IRMPD) experiments with RDX[8] in which the dissociation channels were measured. Decomposition in the condensed phase

$$H_2C{=}N{-}NO_2 \xrightarrow{(0.65)} HCN + HONO$$
$$H_2C{=}N{-}NO_2 \xrightarrow{(0.12)} N_2O + H_2CO$$

does not proceed along the pathway to form HONO and HCN. One possible explanation for this difference is that water formed during the decomposition and retained in the particles may preferentially catalyze the decomposition of methylenenitramine to CH_2O and N_2O. Quantum chemical calculations[15] have shown that hydrolysis of methylenenitramine

(14) Suryanarayana, B.; Graybush, R. J.; Autera, J. R. *Chem. Ind. (London)* **1967**, 2177.

(15) Melius, C. F. Thermochemical Modeling: I. Application to Decomposition of Energetic Materials. In *Chemistry and Physics of Energetic Materials*; Bulusu, S. N., Ed.; Proceedings of the NATO Advanced Study Institute, Vol. 309; Kluwer Academic Publishers: Dordrecht, The Netherlands, 1990; p 21.

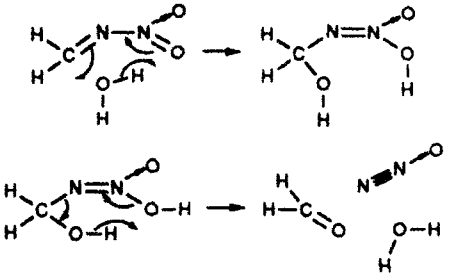

is a lower energy decomposition pathway than unimolecular decomposition. This pathway is also consistent with our observed scrambling of ^{13}C and ^{18}O in the formation of CH_2O from the mixture of HMX-^{13}C/HMX-^{18}O. However, the ^{13}C and ^{18}O also can scramble between the formaldehyde molecules while they are retained in the particles either by forming a formaldehyde polymer and exchanging the carbon and oxygen upon decomposition of the polymer or by undergoing an aldehyde hydration/dehydration process, thus exchanging the oxygen between the water and formaldehyde.

The isotopic scrambling results for NMFA and ONTNTA provide more insight into the possible reactions that control the first step of the HMX decomposition. The results from the HMX-^{13}C/HMX-$^{15}N_{ring}$ show that only one of the C–N bonds in NMFA results from mixing of the isotopes from the two different HMX analogues. This result is consistent with the unimolecular decomposition mechanism based on least-energy pathways of reaction R1.[7] The H_2CN radical, formed in reaction R1, may react with formaldehyde that is trapped within the particles to form the $H_2CNHCHO$ radical which then may abstract a hydrogen atom to form NMFA. This mechanism for the formation of NMFA is consistent with the isotopic scrambling results and also the appearance of NMFA only after formaldehyde becomes available for reaction within the particles.[4] Even though the results cannot identify which C–N bond in NMFA does not break during its formation, it appears more likely that the H_3C–N bond is from the HMX molecule and that the N–CHO bond is formed during the reaction. The possibility that the C–N–C bond structure is from the original molecule is precluded by the scrambling of only one C–N bond in the formation of the NMFA.

The fact that only about 25% of the ONTNTA formed from HMX-ul/HMX-$^{15}N_8$ is a mixed-isotope product argues against a mechanism in which the NO_2 is replaced by an NO molecule trapped in the particle

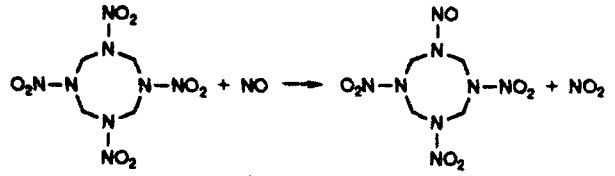

It suggests either that the ONTNTA is formed by a bimolecular reaction with an adjacent HMX molecule or that the N–N bond breaks to form NO_2 which is then trapped in a cage in the HMX lattice.[16] Once trapped in the cage the NO_2 may either re-form the N–N bond or react with the atoms from the molecules forming the "wall" of the cage. The NO_2 may abstract a hydrogen atom from one of the surrounding molecules, forming HONO. The HONO may react with the HMX radical remaining after the fission of the N–N bond to form ONTNTA and an OH radical. The OH radical may then react with an adjacent HMX molecule and abstract a hydrogen atom, forming water and initiating the decomposition of the HMX molecule.[7] Alternatively, ONTNTA may be formed by a bimolecular reaction between two adjacent HMX molecules, in which an oxygen atom on a nitro group abstracts a hydrogen from the adjacent HMX molecule, forming an OH radical and causing the adjacent molecule to decompose. The observed DKIE would be consistent with this alternative route.

The thermal decomposition experiments with HMX-d_8 clearly show a DKIE. The fact that hydrogen atom transfer is involved in a rate-limiting step of HMX decomposition is clearly supported by the formation of water in the two experiments with mixtures of HMX-ul and HMX-d_8. The results from the mechanically mixed HMX sample show that the water formed during the early stages of the experiment is formed predominantly from HMX-ul and that the water formed during the later stages is formed mostly from HMX-d_8. (The value of x goes from 2.24 to 1.0.) This shows that the reactions are occurring within the HMX particles and hydrogen transfer is involved in at least one branch of the decomposition reaction. After the water leaves the individual particles, it undergoes complete isotopic scrambling prior to exiting the reaction cell, as indicated by the mixing fraction of 1.0 measured for the mechanically mixed HMX-ul/HMX-d_8 sample.

The ratio of the rates of formation of H_2O to D_2O of 1.36 from the decomposition of the HMX-ul/HMX-d_8 sample that was mixed in acetone solution also supports hydrogen atom transfer in a rate-limiting step of the decomposition reaction. In addition, the high degree of temporal correlation between the H_2O^+, HDO^+, and D_2O^+ signals and the increased rate of decomposition compared to the results of the experiment with the mechanically mixed sample indicates that this rate-limiting step is at least bimolecular. The mixing, on a molecular level, of the unlabeled HMX or its decomposition products with the HMX-d_8 increases the rate of decomposition of the deuterium-labeled analogue. This result together with the autocatalytic-like behavior of the decomposition suggests that the catalyst is a hydrogen-containing compound and that hydrogen transfer involving the catalyst controls at least one branch of the decomposition reaction. It also suggests that the hydrogen-transfer reaction may involve transfer of hydrogen to the HMX molecule rather than abstraction of a hydrogen atom. For if the reaction involves hydrogen abstraction from HMX, then the reaction rate will be controlled by the particular hydrogen isotope on the HMX molecule and the rate of decomposition should show the same behavior as observed in the experiment with the mechanically mixed HMX-ul/HMX-d_8 sample. Alternatively, the increased reaction rate of the sample mixed in acetone solution compared to that of the mechanically mixed sample may be due to the better dispersion of the catalyst generated from the unlabeled HMX with the remaining sample. Thus, a larger reaction interface may be created between the catalyst that is generated faster from the unlabeled HMX and the remaining HMX for the sample mixed in acetone. Neither hydrogen attack on the HMX molecule nor an increased reaction interface can be eliminated as an explanation of the DKIE based on the data.

A branch of the reaction mechanism that is consistent with the observed DKIE is the hydrolysis of HMX as originally proposed by *Melius*[15]

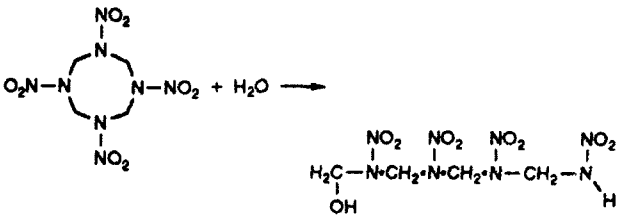

followed by the water-catalyzed decomposition of the hydrolyzed intermediate by

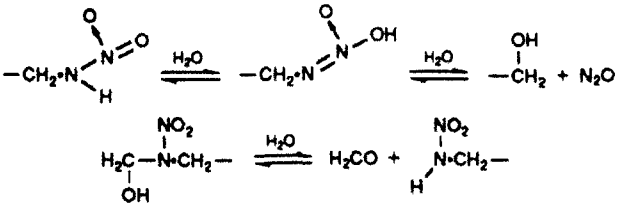

to form the N_2O and CH_2O products.

(16) Fifer, R. A. In *Proceedings of the 19th JANNAF Combustion Meeting, Greenbelt, MD, Oct 1982*; Publ. 366; Chem Propulsion Information Agency, John Hopkins University, Applied Physics Laboratory: Laurel, MD; Vol. I, p 311.

Since the γ-polymorph of HMX is known to crystallize with water of hydration (2 mol of HMX, 0.5 mol of H_2O), experiments utilizing γ-HMX formed by precipitating HMX in $H_2{}^{18}O^{17,18}$ were performed to determine whether the oxygen-18 from the water trapped in the γ-HMX lattice would be incorporated into the formaldehyde formed during the decomposition. Unfortunately, the water was expelled from the sample between 120 and 185 °C and was not available to participate in the reaction when the HMX started to decompose.

Summary and Conclusions

Thermal decomposition experiments with deuterium, ^{13}C, ^{15}N, and ^{18}O isotopic analogues of HMX have been used to investigate the decomposition mechanism of HMX. By determining the extent of isotopic scrambling in each decomposition product and examining the DKIE on the rates of formation of the various products, we have drawn several conclusions about the HMX decomposition mechanism. First, the reaction pathway in which the N–N bond breaks forming NO_2, H_2CN, and three methylenenitramine intermediates that subsequently decompose into CH_2O and N_2O is consistent with the lack of hydrogen isotope scrambling in CH_2O, the lack of nitrogen isotopic scrambling in N_2O, and the scrambling of only one C–N bond in the formation of NMFA. Second, the DKIE clearly shows that there is another decomposition channel in which the rate-limiting step involves hydrogen atom transfer. Comparison of differences in the DKIE in experiments run on mixtures of HMX-ul and HMX-d_8 that were mixed either mechanically or in solution suggests that the reaction mechanism involves transfer of a hydrogen atom to the HMX rather than abstraction of hydrogen from the HMX. Third, the lack of complete isotopic scrambling of the N–NO bond in ONTNTA shows that some decomposition does occur in the HMX lattice and that a cage effect[15] may play some role in the decomposition of HMX. Finally, the results are consistent with an autocatalytic mechanism in which water trapped within the HMX particles acts as the catalyst. The results show that the decomposition of HMX in the condensed phase is a complex process that involves several different reaction branches.

Acknowledgment. The authors thank M. G. Mitchell for assistance in running the experiments and collecting the data and J. R. Autera for assistance in the isotopic syntheses. Research was supported in part by a joint Memorandum of Understanding between the U.S. DOE and the U.S. Army and by the U.S. Army Research Office.

(17) Main, P.; Cobbledick, R. E.; Small, R. W. H. *Acta Crystallogr.* **1985**, *C41*, 1351.

(18) Cady, H. H.; Smith, L. C. Studies on the Polymorphism of HMX. Report No. LAMS-2652; Los Alamos Scientific Laboratory: University of California, 1961.

DISTRIBUTION LIST

Commander
Armament Research, Development and Engineering Center
U.S. Army Armament, Munitions and Chemical Command
ATTN: SMCAR-IMI-I (3)
SMCAR-AEE (3)
SMCAR-AEE-B (5)
Picatinny Arsenal, NJ 07806-5000

Commander
U.S. Army Armament, Munitions and Chemical Command
ATTN: AMSMC-GCL (D)
Picatinny Arsenal, NJ 07806-5000

Administrator
Defense Technical Information Center
ATTN: Accessions Division (12)
Cameron Station
Alexandria, VA 22304-6145

Director
U.S. Army Material Systems Analysis Activity
ATTN: AMXSY-MP
Aberdeen Proving Ground, MD 21005-5066

Commander
Chemical Research, Development and Engineering Center
U.S. Army Armament, Munitions and Chemical Command
ATTN: SMCCR-MSI
Aberdeen Proving Ground, MD 21010-5423

Director
U.S. Army Edgewood Research, Development and Engineering Center
ATTN: SCBRD-RTT (Aerodynamics Technical Team)
Aberdeen Proving Ground, MD 21010-5423

Director
Ballistic Research Laboratory
ATTN: AMXBR-OD-ST
Aberdeen Proving Ground, MD 21005-5066

Chief
Benet Weapons Laboratory, CCAC
Armament Research, Development and Engineering Center
U.S. Army Armament, Munitions and Chemical Command
ATTN: SMCAR-CCB-TL
Watervliet, NY 12189-5000

Commander
U.S. Army Rock Island Arsenal
ATTN: SMCAR-TL, Technical Library
Rock Island, IL 61299-5000

Director
U.S. Army TRADOC Systems Analysis Activity
ATTN: ATAA-SL
White Sands Missile Range, NM 88002